



# DUAL-ANNULAR SLOT PHASE-SHIFTING CELL LOADED WITH MEMS SWITCHES FOR RECONFIGURABLE REFLECTARRAYS

Tony Makdissy, Raphaël Gillard, Erwan Fourn, Etienne Girard, Hervé Legay

## ► To cite this version:

Tony Makdissy, Raphaël Gillard, Erwan Fourn, Etienne Girard, Hervé Legay. DUAL-ANNULAR SLOT PHASE-SHIFTING CELL LOADED WITH MEMS SWITCHES FOR RECONFIGURABLE REFLECTARRAYS. 33rd ESA antenna workshop on challenges for space antenna systems, Oct 2011, Netherlands. 2011. <hal-00772534>

**HAL Id: hal-00772534**

**<https://hal.archives-ouvertes.fr/hal-00772534>**

Submitted on 10 Jan 2013

**HAL** is a multi-disciplinary open access archive for the deposit and dissemination of scientific research documents, whether they are published or not. The documents may come from teaching and research institutions in France or abroad, or from public or private research centers.

L'archive ouverte pluridisciplinaire **HAL**, est destinée au dépôt et à la diffusion de documents scientifiques de niveau recherche, publiés ou non, émanant des établissements d'enseignement et de recherche français ou étrangers, des laboratoires publics ou privés.

# DUAL-ANNULAR SLOT PHASE-SHIFTING CELL LOADED WITH MEMS SWITCHES FOR RECONFIGURABLE REFLECTARRAYS

T. Makdissy<sup>(1)</sup>, R. Gillard<sup>(1)</sup>, E. Fourn<sup>(1)</sup>, E. Girard<sup>(2)</sup>, H. Legay<sup>(2)</sup>

<sup>(1)</sup>*Institute of Electronics and Telecommunications of Rennes IETR, INSA of Rennes  
20, Avenue des buttes de Coësmes, CS 70839, 35708 Rennes Cedex 7, France  
{tony.makdissy, raphael.gillard, erwan.fourn}@insa-rennes.fr*

<sup>(2)</sup>*Thales Alenia Space, 26 Avenue Jean François Champollion, 31037 Toulouse Cedex 1, France  
{etienne.girard, herve.legay}@Thalesaleniaspace.com*

## 1. ABSTRACT

Reconfigurable reflectarrays require low-loss and low-dispersion active cells in order to achieve efficient beam scanning or beam shaping on a large bandwidth. The low-loss constraint is the more stringent as the introduction of tunable components (such as MEMS) in resonant phase-shifting cells may dramatically decrease their quality factor. In this paper, a comprehensive review of recent developments at IETR and TAS is carried out with the objective to dynamically control complementary resonant modes in a reconfigurable phase-shifting cell. The new topology consists of a dual-annular slot loaded with 8 MEMS switches. It operates around 12 GHz and can provide four equidistributed phase states with low dispersion and low losses.

## 2. INTRODUCTION

Reflectarray cells usually use planar resonant elements (either patch or slot) to vary the phase of the reflected wave. By modifying the resonant element (either its geometry for passive cells or its loading for active ones), the resonant frequency can be changed and so the reflected phase.

Basically, two types of resonators can be used: patch resonators exhibit a series resonance with a 180° phase shift at resonance while slot resonators involve a shunt resonance with a 0° phase shift at resonance.

It is well known that a single resonance is usually not sufficient to achieve full 360° phase coverage. As a consequence, multiple resonators are advantageously used to increase the overall phase range, up to twice or three times the required 360° value [1, 2]. This also makes possible to use smoother resonances leading to both reduced losses and better fabrication tolerances when successive resonances are displaced simultaneously.

By combining different resonators on a single layer, the phase range can be increased while preserving a simple technological process, leading to a low-cost antenna. In [3], a slot-loaded patch was proposed that supports both a patch and a slot resonance. In [4], two concentric cross loops were used providing successive resonances with a single dielectric substrate. Most of these concepts have been extended to active structures. To do so, the slots

are controlled by MEMS switches thus providing a dynamical tuning of the reflected phase [5].

Unfortunately, in all these examples, the phase variation is dominated by the resonant behavior of the structure. More precisely, most of the phase range results from applied perturbations to one or several resonant mode(s). Consequently, as the structure always operates close to its resonance(s), it is basically dispersive and dissipative.

In this paper, we propose to use an alternative approach where we try to operate far from the resonances of the structure. By doing so, we naturally benefit from smooth variations of the phase. However, this alone would not permit to achieve full 360° phase coverage. Next, the idea is to switch between two complementary resonance mechanisms, each providing a different phase coverage: a slot mode, i.e. shunt resonance, will be used to achieve a phase range opposite to 0° (typically from 90° to 270°) while a patch mode, i.e. series resonance, (or ring mode depending on the topology of the metallization) will be used to achieve the complementary phase range (from -90° to 90°). In both cases, the chosen mode is used out of its natural resonance domain, which permits to prevent from any high losses. The concept is applied to a planar active cell where the switching between a quasi ring mode and the slot mode is obtained thanks to MEMS components.

## 3. CRITICAL REVIEW OF PREVIOUS CELL DESIGNS

Several active cells have been developed during the last ten years by TAS and IETR with the objective to achieve a large bandwidth on a single dielectric substrate. In a preliminary version [5], the cell was a simple extension of the slot-loaded patch concept [3]. MEMS switches were used to control both the size of the patch and of the loading slots. Although the phase range complied with the 360° requirement, the frequency dispersion was quite high as both resonators (patch and slot) were used close to their resonances. In addition, the cell size was quite large (>0.6 lambda) which is not appropriate for large beam deviations.

An updated version was obtained by using several concentric metallic rings and by loading the slots in

between with MEMS switches [6]. This structure has three main advantages. Firstly, the ring is a more compact configuration than the patch resulting in a smaller inter-element spacing (typically less than a half wavelength). Secondly, the availability of numerous resonators increases the achieved phase range. Finally, this structure is very versatile as it offers many degrees of freedom. Consequently, it can behave as a multiple-slot resonator or as a multiple-ring resonator depending on the activated MEMS switches. However, these advantages are obtained at the expense of an increased complexity. In practice, the analysis of the involved resonating modes is quite tough and the optimization of the design (both the dimensions of the metallic structure and the location of the MEMS components) appears as a cumbersome and quite empirical task. So, specific optimization tools were developed to minimize the number of MEMS controls while taking advantage of the capability of this structure to provide the same phase with different MEMS configurations [7]. Along this process, it was also discovered that some phase states were associated with high-order resonant modes and could be highly dissipative. The problem could however be overcome by *a priori* elimination of the more dispersive states using intensive simulations. As a result, an optimized cell with 8 MEMS switches was obtained [6] (Fig. 1). Its characteristic table relating phase shifts to MEMS configurations is quite regular and linear (Fig. 2). Furthermore, by eliminating MEMS configurations with highly dispersive behaviours, the bandwidth (defined for a gain reduction less than 1 dB) has been increased from 3 to 14% (Fig. 3).

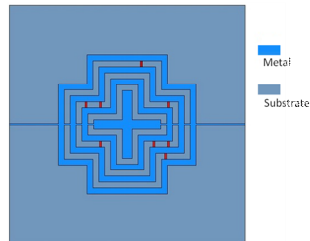


Figure 1. Optimized cell

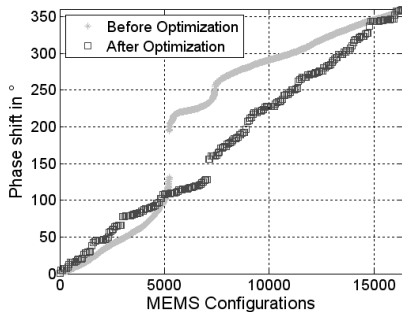


Figure 2. Cell's characteristic table

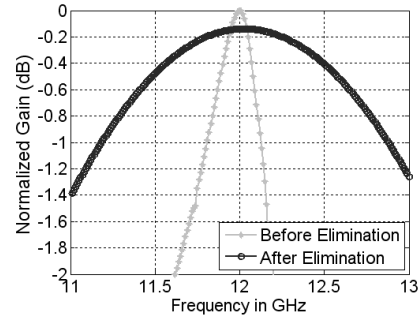
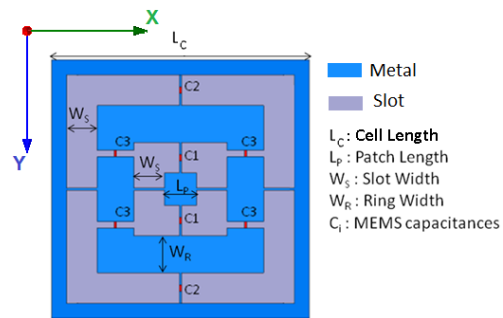


Figure 3. Normalized gain versus frequency

In spite of these quite promising performances, the empirical approach that was used to optimize the design was not really satisfactory as it did not rely on a full understanding of the complex resonant mechanisms within the structure when MEMS switches were activated. However, a deeper *a posteriori* insight suggests that the main interest of the design is the combination of slot and ring modes in a single structure. Smooth phase variations close to  $0^\circ$  can be achieved when a ring mode is involved, provided its resonant frequency is sufficiently distant from the considered band of operation. Conversely, smooth phase variations close to  $180^\circ$  can be obtained with a slot mode far from its resonant frequency. For intermediary phase states, it seems a smooth evolution can only be preserved if at least two modes of the same type (either slot or ring) are varied simultaneously. Similar conclusions have also been carried out by analyzing the so-called Phoenix cell [8]. From these experiences, a more systematic methodology can be introduced to derive a new design.

#### 4. AN IMPROVED ACTIVE CELL

The new cell is depicted in Fig. 4. It basically consists of two square-annular slots within a ground plane. In the following, it is assumed that the cell is excited by a vertically-polarized incident wave (electric field parallel to y-axis) with normal incidence and operates around 12 GHz. It is simulated using HFSS with Floquet boundary conditions. Three sets of MEMS capacitances  $C1$ ,  $C2$  and  $C3$  are used to control the geometry of the cell.



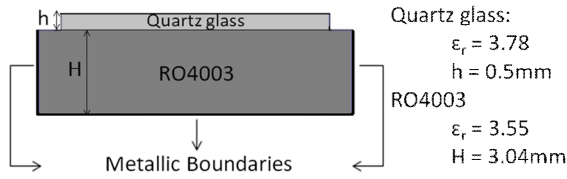


Figure 4. Phase shifting cell loaded with MEMS capacitances and the double layer substrate

$C1$  and  $C2$ , in the open-circuit plane of the slots, are used to load the inner and outer slots respectively. When their value is increased, the electric length of the associated slot gets higher and consequently its resonant frequency is decreased [9]. As a consequence, the simultaneous variation of  $C1$  and  $C2$  provides a convenient way of controlling two successive slot modes. As explained in the previous section, it aims at providing intermediate phase states with low dispersion.  $C3$  is used to load the metallic ring separating the slots. When  $C3$  is high, the cell behaves as two square-annular slots. On the contrary, when  $C3$  is low, only the horizontal parts of the slots are active, as can be seen in Fig. 5.

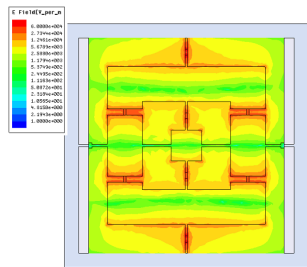


Figure 5. Electric field mapping for  $C3$  low (20fF)

Indeed, the main operating modes of the cell can be interpreted using the equivalent electric circuit shown in Fig. 6. It consists of the series connection of two shunt resonators, each of which corresponding to one of the slots. Such a circuit exhibits two anti-resonances (shunt resonances) and one (series) resonance in between. The two anti-resonances are due to the slots while the resonance is mainly related to the metallic ring. As explained before,  $C1$  and  $C2$  mainly control the resonant frequencies of the slots while  $C3$  mainly affects that of the ring. As a consequence, these capacitances altogether provide an efficient means of modulating the different resonant modes in the structure. However, it should be emphasized that modes are tightly coupled and cannot really be dealt with independently. For instance, it seems obvious a pure ring resonance is not possible alone as the ring itself is printed inside a slot. This means the ring resonance always ends as a slot resonance, as can be understood from Fig. 6.

Nonetheless, the versatility of the structure offers numerous possibilities to adjust the reflected phase range. For instance, when the slot resonances are pushed

apart, a flat zone is obtained in-between, providing smooth variations with phase values close to  $180^\circ$ . On the contrary, to achieve phase values close to  $0^\circ$ , one of the slot resonant frequencies has to be moved towards the operating frequency.

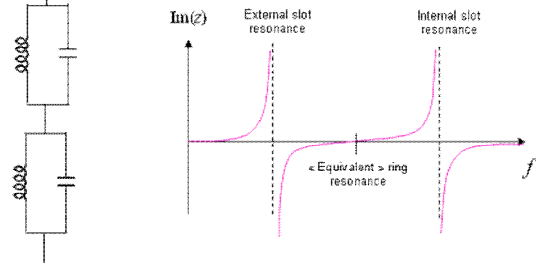


Figure 6. Equivalent electric circuit of the cell

Fig. 7 to 9 present some of the various possible operating modes.

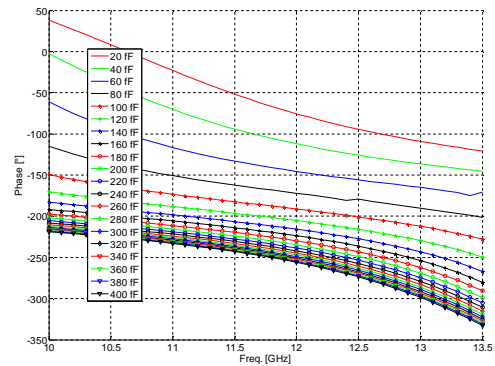


Figure 7. Phase versus frequency for  $C3 = 20fF$ , and simultaneous variation of  $C1$  and  $C2$  ( $L_C=12mm$ ,  $L_P=1.5mm$ ,  $W_S=1.425mm$ ,  $W_R=1.7mm$ )

In Fig. 7,  $C3$  is low and  $C1$  and  $C2$  are varied simultaneously. A  $[-70^\circ, -260^\circ]$  phase range with very low variations (dispersion lower than  $-45^\circ/GHz$ ) can be observed at 12 GHz.

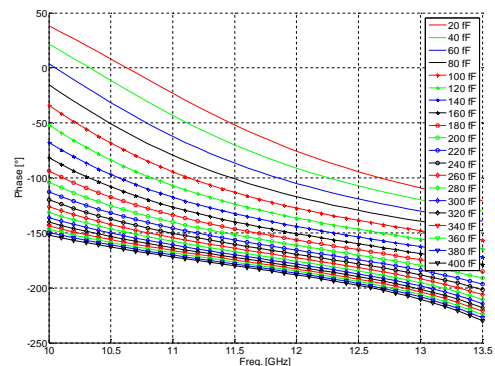


Figure 8. Phase versus frequency for  $C3$  variable,  $C1$  and  $C2$  constant equal to 20fF ( $L_C=12mm$ ,  $L_P=1.5mm$ ,  $W_S=1.425mm$ ,  $W_R=1.7mm$ )

In Fig. 8,  $C_3$  is varied with  $C_1$  and  $C_2$  close to 0 (20fF). Here again the curves are very smooth but the phase range is not improved.

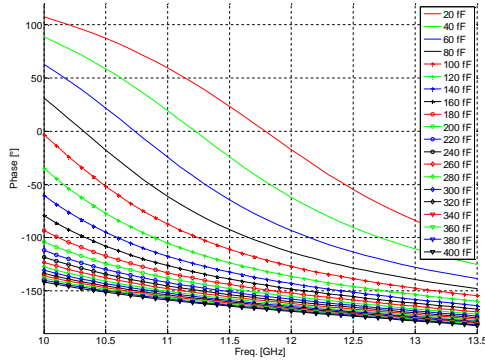


Figure 9. Phase versus frequency for  $C_1 = 400\text{fF}$ ,  $C_2 = 20\text{fF}$  and  $C_3$  variable ( $L_C=12\text{mm}$ ,  $L_P=1.5\text{mm}$ ,  $W_S=1.425\text{mm}$ ,  $W_R=1.7\text{mm}$ )

In Fig. 9, a fixed high value of  $C_1$  (400fF) and a fixed low value of  $C_2$  (20fF) are combined with a progressive variation of  $C_3$ . This mode provides phase curves close to  $0^\circ$  completing the overall phase coverage. However, the associated dispersion is not as low as in the previous cases. This is due to the fact that no pure ring mode can be excited alone, as explained before.

Finally, 4 uniformly-distributed phase states have been selected from all the available phase curves (Fig. 7 to Fig. 9) and are reported in figure 10.

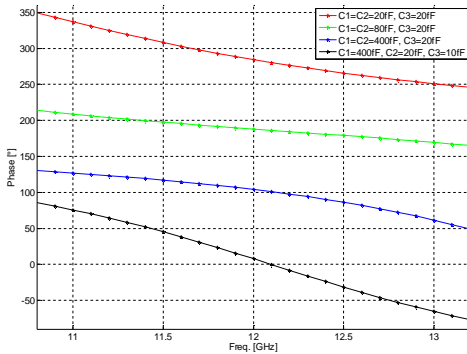


Figure 10. Four uniformly-distributed Phase States

The four phases provided at the central frequency of 12 GHz are respectively:  $7^\circ$ ,  $104^\circ$ ,  $188^\circ$  and  $284^\circ$ . According to the phase standard deviation criterion (bandwidth for phase standard deviation  $< 31^\circ$ ) [10] we note that the bandwidth achieved is 20% around 12GHz, from 10.8 GHz to 13.2 GHz (Fig. 11). A 1.98-bit phase-shifter is obtained.

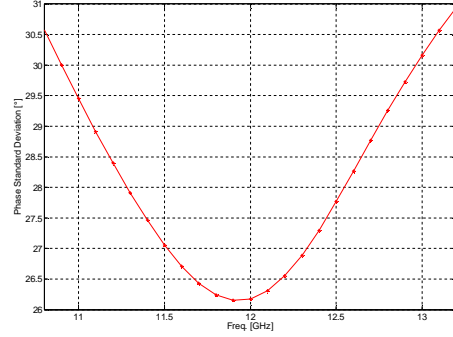


Figure 11. Phase standard deviation versus frequency

Fig. 12 presents the associated loss. It is less than 0.3dB over the whole bandwidth.

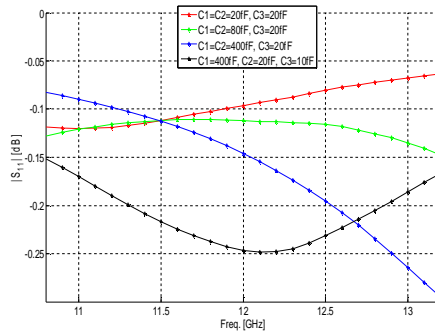


Figure 12. Module of reflection coefficient versus frequency for the four selected configurations

At the central frequency of 12 GHz, the maximum loss is associated to the configuration with the maximum frequency dispersion ( $-77^\circ/\text{GHz}$ ).

## 5. CONCLUSIONS

A new dual-annular slot phase-shifting cell loaded with MEMS capacitances has been designed. A comprehensive study has been proposed relying on an equivalent electric circuit. MEMS capacitances permit to switch between slot modes and a quasi ring mode, used out of their respective resonance. As a result, very smooth phase variations have been demonstrated, for all phase values, except around  $0^\circ$  where dispersion is a bit higher due to the impossibility to excite a pure series resonance. The covered phase range when slot mode is active is  $190^\circ$ , the complementary phase range is provided when the other mode is excited. With a suitable selection, four equidistributed phase states were provided with 0.25dB of maximum losses at the central frequency of 12 GHz and 20% of bandwidth

## 6. ACKNOWLEDGMENTS

Most of these developments have been supported by ESA within the MERCURY project

## 7. REFERENCES

1. J. Encinar, "Design of two-layer printed reflectarrays using patches of variable size," *IEEE Trans. Antennas Propag.*, vol. 49, no. 10, pp. 1403-1410, Oct. 2001.
2. J. Encinar and J. Agustin Zornoza, "Broadband design of three-layer printed reflectarrays," *IEEE Trans. Antennas Propag.*, vol. 51, no. 7, pp. 1662-1664, Jul. 2003.
3. D. Cadoret, A. Laisne, R. Gillard, L. Le Coq, H. Legay, "Design and measurement of a new reflectarray antenna using microstrip patches loaded with a slot," *Electronic Letters*, vol. 41, no. 11, pp. 623-624, 2005.
4. M.R. Chahamir et al., "Broadband reflectarray antenna with double cross loops," *Electronic Letters*, 2006, vol. 2, pp. 65-66.
5. H. Legay, G.Caille, P.Pons, E. Perret, H. Aubert, J. Pollizi, A. Laisne, R. Gillard, M. Van Der Worst, "MEMS controlled phase-shift elements for a linear polarized reflectarray," in *28<sup>th</sup> ESA Antenna Technology Workshop on Space Antenna Systems Technologies*, Netherlands, pp. 443-448, 20-31 May 2005.
6. H. Salti, E. Fourn, R. Gillard, E. Girard, H. Legay, "'Pharmacist Cross' phase-shifting cell loaded with MEMS switches for reconfigurable reflectarrays," *European Conference on Antennas and Propagation EUCAP 2010*, Barcelona, 12-16 April 2010.
7. H. Salti et al., "Robustness optimization of MEMS-based reflectarray phase-shifting cells," *European Conference on Antennas and Propagation EUCAP 2009*, Berlin, pp. 3742 – 3728, 23-27 March 2009.
8. L. Moustafa, R. Gillard, F. Peris, R. Loison, H. Legay, E. Girard, "The Phoenix Cell: A New Reflectarray Cell With Large Bandwidth and Rebirth Capabilities," *IEEE AWP Lett.*, Vol. 10, 2011, pp. 71-75.
9. M. Kharbech, R. Gillard, R. Loison, H. Legay, E. Girard, "Compact frequency agile slot ring resonators for reflectarray phase shifting cells," *European Conference on Antennas and Propagation EUCAP 2011*, Rome, pp. 2113 – 2116, 11-15 April 2011.
10. R. Pereira, R. Gillard, R. Sauleau, P. Potier, T. Dousset, X. Delestre, "Dual Linearly-Polarized Unit-Cells With Nearly 2-Bit Resolution For Reflectarray Applications In X-Band," *IEEE Trans. On AP*, under review.